

PRELIMINARY RESULTS OF BTDF CALIBRATION OF TRANSMISSIVE SOLAR DIFFUSERS FOR REMOTE SENSING

Georgi T. Georgiev^{1*}, James J. Butler², Kurt Thome², Catherine Cooksey³, Leibo Ding¹

¹Science Systems and Applications, Inc., Lanham, MD 20706,

²Biospheric Sciences Branch, NASA Goddard Space Flight Center, Greenbelt, MD 20771

³National Institute of Standards and Technology, Gaithersburg, MD 20899

*Corresponding author: georgi.t.georgiev@nasa.gov

ABSTRACT

Satellite instruments operating in the reflected solar wavelength region require accurate and precise determination of the optical properties of their diffusers used in pre-flight and post-flight calibrations. The majority of recent and current space instruments use reflective diffusers. As a result, numerous Bidirectional Reflectance Distribution Function (BRDF) calibration comparisons have been conducted between the National Institute of Standards and Technology (NIST) and other industry and university-based metrology laboratories. However, based on literature searches and communications with NIST and other laboratories, no Bidirectional Transmittance Distribution Function (BTDF) measurement comparisons have been conducted between National Measurement Laboratories (NMLs) and other metrology laboratories. On the other hand, there is a growing interest in the use of transmissive diffusers in the calibration of satellite, air-borne, and ground-based remote sensing instruments. Current remote sensing instruments employing transmissive diffusers include the Ozone Mapping and Profiler Suite instrument (OMPS) Limb instrument on the Suomi-National Polar-orbiting Partnership (S-NPP) platform, the Geostationary Ocean Color Imager (GOCI) on the Korea Aerospace Research Institute's (KARI) Communication, Ocean, and Meteorological Satellite (COMS), the Ozone Monitoring Instrument (OMI) on NASA's Earth Observing System (EOS) Aura platform, the Tropospheric Emissions: Monitoring of Pollution (TEMPO) instrument and the Geostationary Environmental Monitoring Spectrometer (GEMS). This ensemble of instruments requires validated BTDF measurements of their on-board transmissive diffusers from the ultraviolet through the near infrared. This paper presents the preliminary results of a BTDF comparison between the NASA Diffuser Calibration Laboratory (DCL) and NIST on quartz and thin Spectralon samples.

Keywords: BRDF, BRDF, Calibration, Spectralon, Reflectance, Remote Sensing.

1. INTRODUCTION

The study of Earth's geophysical processes requires consistent long-term calibration of the instruments used in the production of Earth remote sensing data¹. Satellite remote sensing instruments operating in the ultraviolet (UV), visible (VIS), near infrared (NIR) and shortwave infrared (SWIR) wavelength regions are an important subset of the instruments required to monitor the Earth. Traditionally, diffuser standards are used in the pre-flight and on-orbit calibration of the radiance responsivity of satellite instruments through measurements of their Bidirectional Scatter Distribution Function (BSDF). BSDF is a term which includes the Bidirectional Reflectance Distribution Function (BRDF) or the Bidirectional Transmittance Distribution Function (BTDF) depending on instrument deployment scenario. The BSDF is a function of wavelength and geometry and reflects the structural and optical properties of the diffuser. Airborne and ground-based instruments used in the validation of satellite measurements also use diffuse scatter standards as radiometric calibration sources.

In this study, BTDF measurements were performed on transmissive quartz and Spectralon samples at NASA's Goddard Space Flight Center (GSFC) Diffuser Calibration Laboratory (DCL) using an out-of-plane optical scatterometer. The DCL has served as a secondary calibration facility for over two decades with NIST as the primary calibration facility. The DCL has provided numerous NASA projects with BSDF data in the UV, VIS and the NIR spectral regions. Historically, NIST traceability of GSFC optical BRDF measurements is established and maintained using sets of diffuse reflective Spectralon* laboratory standards measured yearly by NIST on their Spectral Tri-function Automated Reference Reflectometer (STARR) and before all customer project measurements by GSFC. We have expanded the DCL traceability to NIST for BTDF in this work by reporting BTDF cross calibration measurements with NIST on two transmissive laboratory standards.

2. INSTRUMENTATION

The scatterometer, as shown in Fig.1, used currently for BSDF measurements covers the spectral range from 230 nm to 1.1 μm . Although more detailed information on the scatterometer is published elsewhere² we would like to mention some basic parameters. The scatterometer operates using one of two light sources: (i) the broadband monochromator-based source is a 75 W Xenon lamp coupled to a Chromex* 0.25 m monochromator with selectable spectral bandwidth from 0.6 nm to 12 nm and (ii) single wavelength and tunable coherent laser light sources. The scatterometer detector field-of-view is under filled by the incident beam. The angle of the incident beam is determined in the zenith or elevation direction, θ_i , by rotation of the vertical optical table. The position of the receiver is described by the scatter zenith, θ_s , and scatter azimuth angle, ϕ_s . The detector can be rotated around the vertical and horizontal axes of the goniometer to any scatter azimuth and scatter zenith angle. The samples are mounted horizontally on the sample stage and aligned with the scatterometer axes of rotation. The motorized sample stage can be moved in the X, Y and Z linear directions. There is also an additional degree of freedom allowing sample rotation in the horizontal plane. This enables BSDF measurements to be made at any incident azimuthal angle, ϕ_i . The scatterometer detector is polarization insensitive and employs either an ultraviolet enhanced silicon photodiode from 230 nm to 1100 nm or an InGaAs photodiode from 900 nm to 2500 nm with output fed to a computer-controlled lock-in amplifier.

The setup facilitates the acquisition of computerized BSDF measurements at different incident and scattered geometries for a complete data acquisition at pre-selected positions and wavelengths. The measurement uncertainty, Δ_{BRDF} , depends on several instrument variables. It was evaluated in accordance with NIST guidelines³ to be less than 1% ($k = 1$)⁴. The facility has participated in several BRDF round-robin measurement campaigns with domestic and foreign calibration institutions in support of Earth and space satellite validation programs⁵. In addition, the BRDF and 8° directional-hemispherical reflection of soil samples, regolith stimulant, and vegetation have been characterized at the facility⁶.

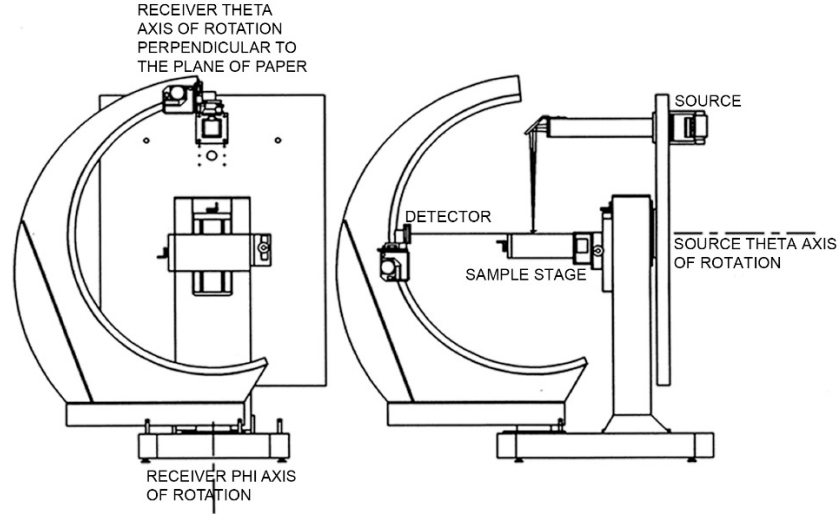


Fig. 1 The DCL Scatterometer

3. METHODOLOGY

We are following the NIST definition of BSDF, according to Nicodemus⁷, in our laboratory calibration measurements. In this case, the BSDF is referred to as the ratio of the scattered radiance, L_s , scattered by a surface into the direction (θ_s, ϕ_s) to the collimated irradiance, E_i , incident on a unit area of the surface:

$$BSDF = \frac{L_s(\theta_i, \phi_i, \theta_s, \phi_s, \lambda)}{E_i(\theta_i, \phi_i, \lambda)}, \quad (1)$$

where θ is the zenith angle, ϕ is the azimuth angle, the subscripts i and s represent incident and scattered directions, respectively, and λ is the wavelength. Nicodemus further assumed that the beam has a uniform cross section, the illuminated area on the sample is isotropic, and all scatter comes from the sample surface.

In practice, we are dealing with real sample surfaces which are not isotropic, and the optical beams used to measure the reflectance are not perfectly uniform. Hence, from practical considerations, the BSDF can be defined, according to Stover⁸, as the scattered power per unit solid angle normalized by the incident power and the cosine of the detector zenith angle. It is expressed in terms of incident power, scattered power and the geometry of incident and reflected light:

$$BSDF = \frac{P_s / \Omega}{P_i |\cos \theta_s|}, \quad (2)$$

where P_s is the scatter power, Ω is the solid angle determined by the detector aperture, A , and the radius from the sample to the detector, R , or $\Omega = A/R^2$, P_i is the incident power, and θ_s is the scatter zenith angle.

The BSDF, f_s , has units of inverse steradians and can range from small numbers (e.g. off-specular black samples) to large values (e.g. highly reflective or transmissive samples at specular geometries). The bidirectional reflectance factor (BRF), R_d , is dimensionless and can be defined in terms of the BRDF as

$$R_d = \pi \cdot BRDF \quad (3)$$

The bidirectional transmittance factor, T_d , the ratio of the BTDF to that of perfectly transmitting diffuser is defined as:

$$T_d = \pi.BTDF , \quad (4)$$

The BSDF as expressed above does not take into account the diffusion of the radiation within the diffuser volume nor does it quantify the impact of the diffuser thickness or the distance between the surface the radiation enters the diffuser and the surface the radiation is emitted. This is particularly important in the case of transmissive diffusers or BTDF calibration measurements. We assert that the irradiance of concern is that on the front surface of the transparent sample. Although the BTDF will then be a function of the thickness of the sample, this is not different from the corresponding specular reflection and specular transmission situations. For now we leave the question of how to interpolate values from one thickness to another, taking note, however, of the problems of bulk scattering, absorption, and the change in solid angle resulting from the refractive index of the material. We do note the additional experimental difficulties of the change in focus of the beam, the multiple surface reflections, and the fact that the beam profile will be measured near the optical axis.

4. MEASUREMENTS

4.1. Directional Hemispherical Transmittance

Presented in this paper are measurements of the Bidirectional Transmittance Distribution Function (BTDF) of diffusers from 290nm to 740nm. We first tested a number of transmissive diffusers in order to identify the best two diffusers to be part of our comparison efforts. The directional hemispherical transmittance of 14 different diffusers was measured in the first round of testing: Three Spectralon diffusers with thicknesses of 100 μm , 250 μm , and 500 μm ; three HOD-500* flame polished diffusers with thicknesses of 15 mm, 5 mm, and 2mm; three HOD-500 grounded diffusers with thicknesses of 15 mm, 5 mm, and 2mm; one HOD mechanically polished diffuser with a thickness of 4 mm; three Diffusil* diffusers, UV500, UV1000, and UV2000 with a thickness of 3mm but different scatter densities; and one Diffusil 500C diffuser with a thickness of 3mm. The HOD-500 and Diffusil diffusers are also referred to as Mie diffusers in this text due to their volume structure. The directional hemispherical reflectance of all 14 samples was measured on the DCL's Perkin Elmer 1050 spectrophotometer and is shown in Fig.2. All three Spectralon samples show a slope increase from the UV to the NIR. The transmittance, as expected, is a function of the sample thickness with the 100 μm highest and the 500 μm lowest. The transmission drops significantly below 300 nm. The grounded HOD-500 diffusers show a much smaller slope increase from the UV to the NIR. When compared to the Spectralon diffusers, their transmittance is less and dependent upon the thickness. The transmission drops even more below 300nm. The flame polished HOD-500 samples show the same slope as the grounded HOD samples but smaller transmittance values, because of the nature of their surface. Also, these diffusers show a higher transmittance in the 200 nm to 300 nm spectral range than the grounded HOD and the Spectralon diffusers. The Diffusil 500C diffuser exhibit very similar hemispherical transmittance properties as the other quartz Mie diffusers. The Diffusil UV-series diffusers are hydroxyl (OH) free and do not exhibit spectral features due to water absorption. Although they are of the same thickness, the directional hemispherical reflectance is proportional to their scatter density as with the UV500 being the highest..

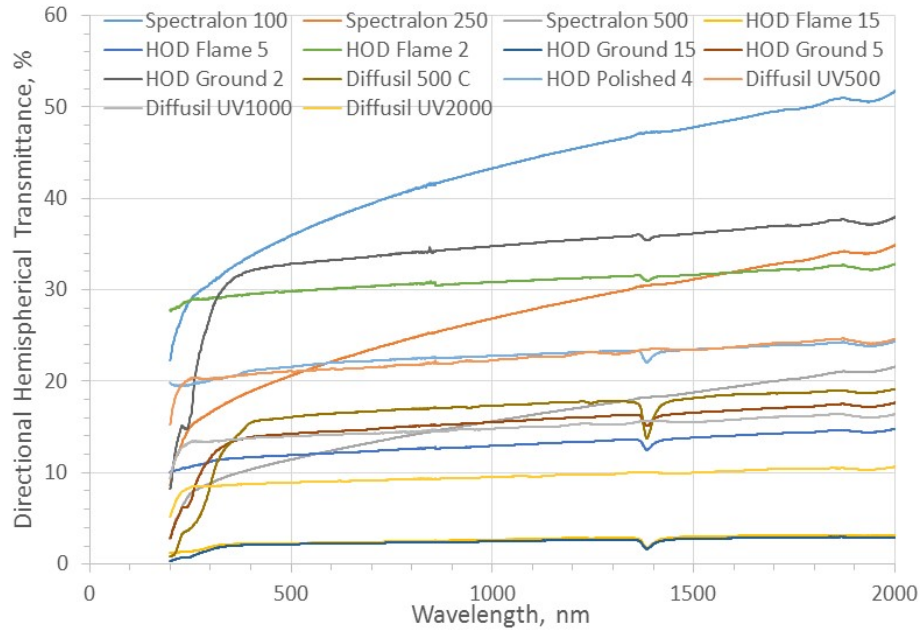


Fig.2. Diffusers Directional Hemispherical Transmittance

4.2. BTDF Measurements

All BTDF measurements are made for polarizations of the illumination beam both parallel, P, and perpendicular, S, to the plane of incidence. The BTDF is fitted for each polarization by dividing the net signal from the reflected radiant flux by the product of the incident flux and the projected solid angle from the calibration item to the limiting aperture of the detector.

The hemispherical transmittance provides a good mark of general performance, but without the angular characterization critical data is missing from many applications and uncertainty budgets. Therefore, the next step in identifying the two GSFC laboratory transmissive standards to be used in the validation of the GSFC NIST traceable BTDF measurement capability is to characterize the transmissive diffusers angular response and provide a full uncertainty budget. Based on the directional hemispherical data already collected we chose the 100 μm Spectralon; 2 mm thick flame polished and grounded and 4 mm thick mechanically polished HOD-500 diffusers; Diffusil 500C, UV500, UV1000 and UV2000 diffusers for further testing. All diffusers were measured in transmission at 633 nm and incident angles $\theta_i=0^\circ$, 45° and 60° ; scatter azimuth $\phi_s=0^\circ$, 90° and 180° ; and scatter zenith θ_s from 110° to 180° in 5° steps. The results summarizing the BTDF of Spectralon, HOD and Diffusil based diffusers are presented in Fig.3.a for Spectralon; Fig.3.b for HOD polished; and Fig.3.c for Diffusil UV500.

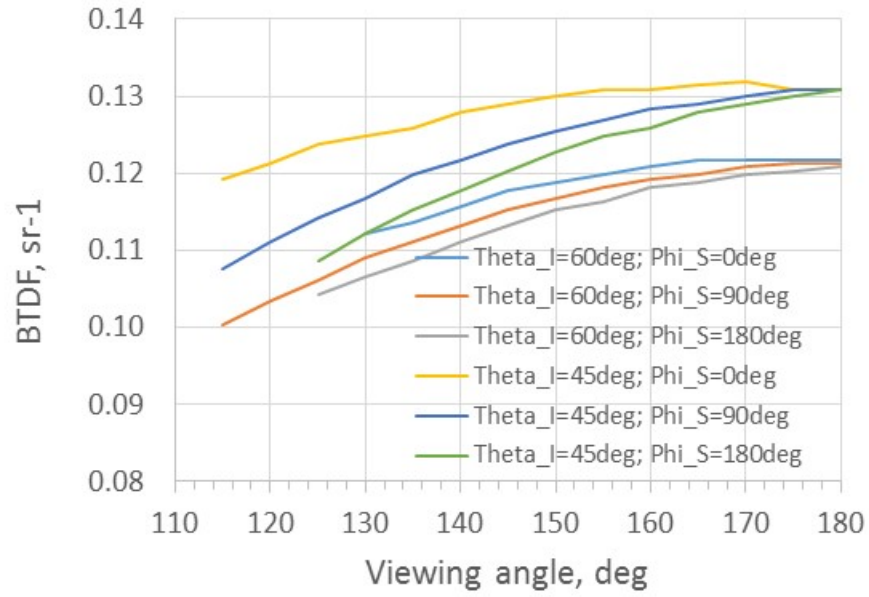


Fig.3.a. BTDF of Spectralon 100 μm , $\theta_i = 60^\circ$ and 45° , $\phi_s = 0^\circ$, 90° , and 180° ; θ_s from 125° to 180° .

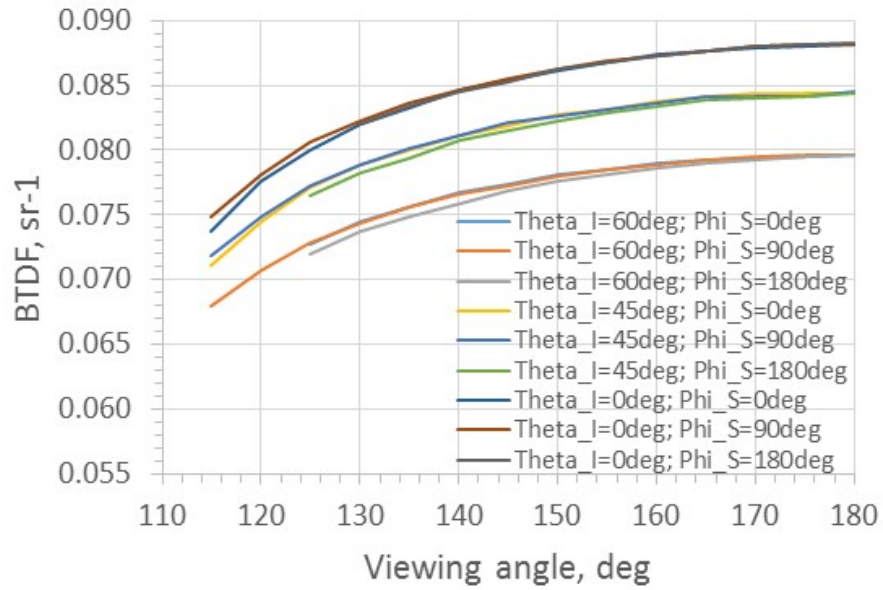


Fig.3.b. BTDF of HOD 4 mm, $\theta_i = 60^\circ$, 45° , and 0° ; $\phi_s = 0^\circ$, 90° , and 180° ; θ_s from 125° to 180° .

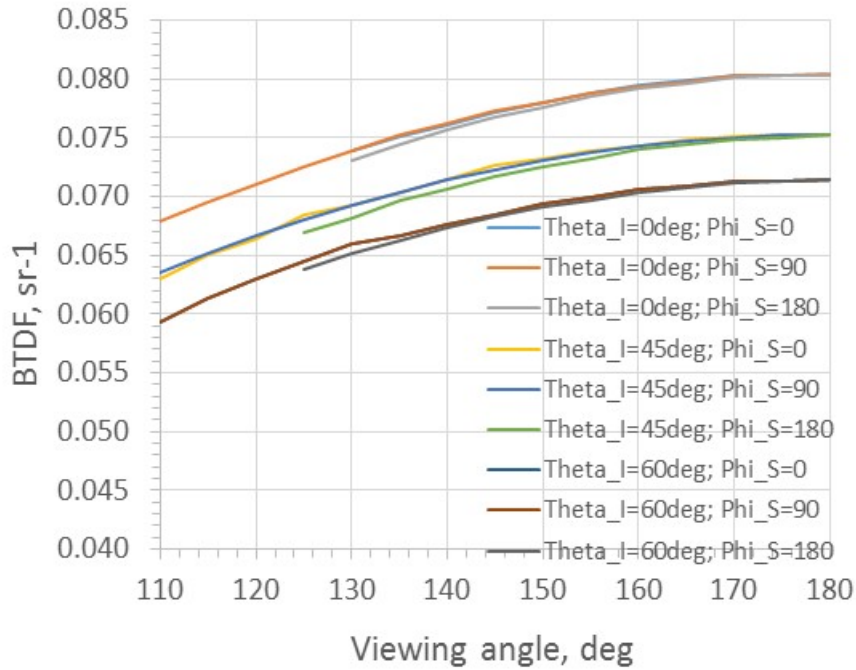


Fig.3.c. BTDF of Diffusil UV500 3 mm, $\theta_i=60^\circ$, 45° , and 0° ; $\phi_s=0^\circ$, 90° , and 180° ; θ_s from 125° to 180° .

With the exception of Spectralon, both HOD and Diffusil diffusers are excellent Lambertian diffusers. The BTDF at forward, backward and out-of-plane scattering directions at a given incident angle has the same or very close values for viewing angles smaller than 160° . Some curves are plotted from the 110° viewing angle but others from 125° due to detector obscuration by the different sample stages used to hold the diffusers. Although not presented here the rest of the tested Diffusil UV1000, UV2000 and HOD diffusers with different thickness show similar scattered light distributions with lower intensities due to material thickness and differing scatter density.

5. RESULTS and DISCUSSION

After thorough analysis of the directional hemispherical transmittance and BTDF data of all tested diffusers and taking into consideration the availability of the diffusers, their physical properties, and instrumental parameters, we selected two transmissive diffusers for further testing and the comparison with NIST. The first was a $250\ \mu\text{m}$ thin Spectralon sample, and the second was $2\ \text{mm}$ thin ground HOD-500 quartz diffuser. We decided to go with the $250\ \mu\text{m}$ Spectralon instead of the previously measured $100\ \mu\text{m}$ as the $100\ \mu\text{m}$ Spectralon on hand did not exhibit a sufficiently flat surface which we assumed may contribute to increased measurement uncertainty. Both diffusers were measured in GSFC's DCL at 7 wavelengths between $250\ \text{nm}$ and $900\ \text{nm}$ and at incident angles of 0° and 30° and scatter angles from 165° to 179° in 2° steps. The same samples were also measured on the NIST STARR instrument at the same geometrical configurations and wavelengths. The validation of our measurements with NIST measurements is shown in Fig.4.a and b for the HOD-500 diffuser at 0° and 30° incident angle and in Fig.4.c and d for the Spectralon diffuser, respectively. All data points are presented in the figures with error bars of 1% ($k=1$) for both NIST and GSFC measurements.

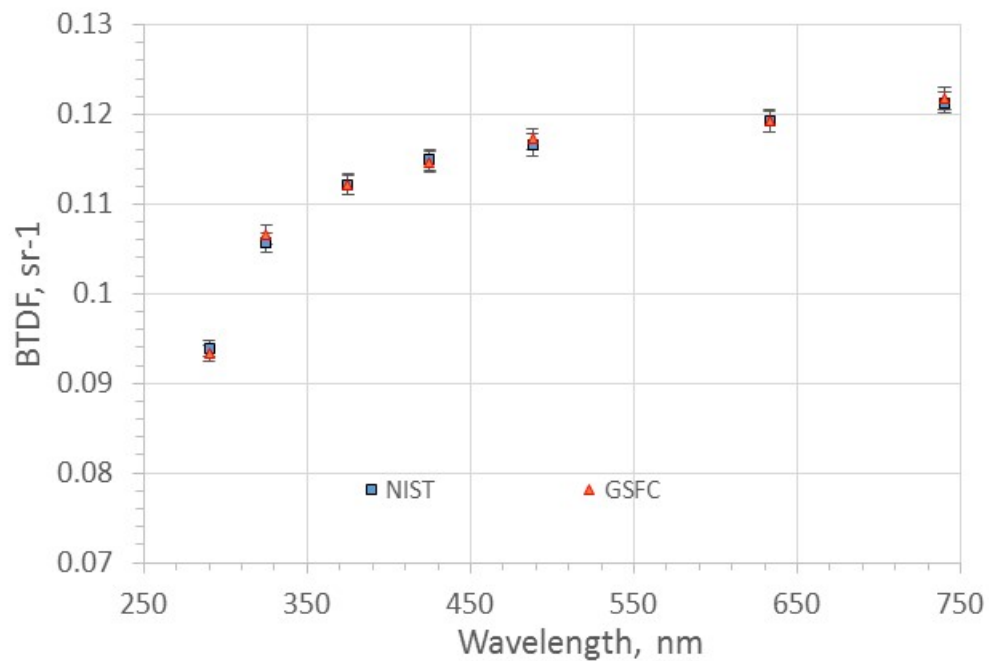


Fig.4.a. BTDF of HOD-500, 2 mm thickness, $\theta_i=0^\circ$, $\theta_s=179^\circ$; $\phi_s=0^\circ$; measured by GSFC and NIST STARR.

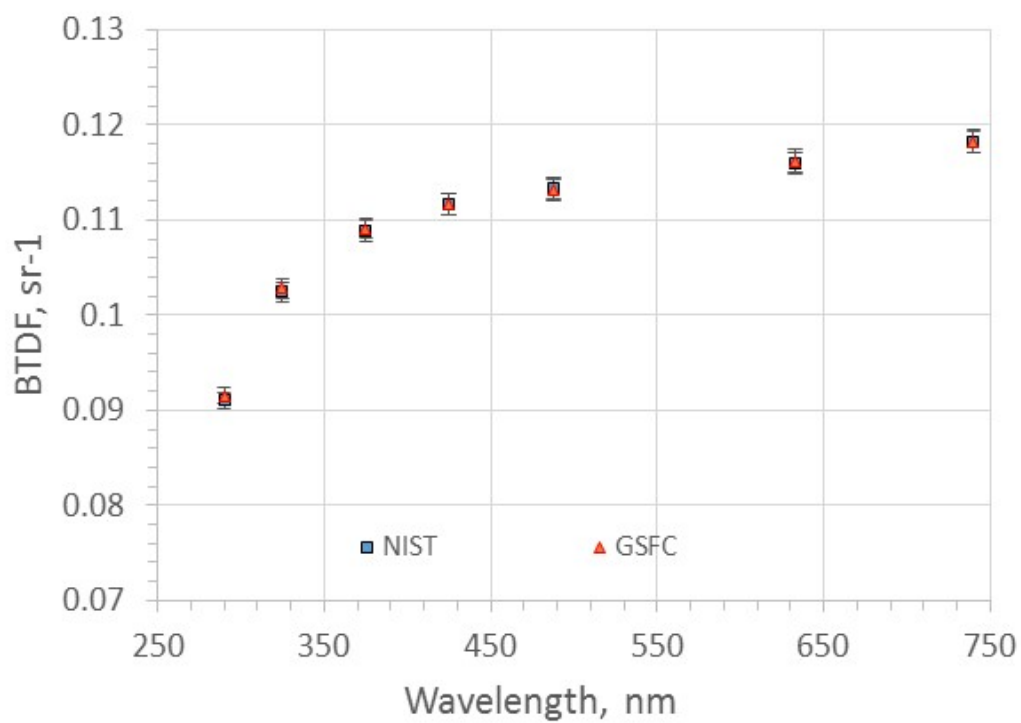


Fig.4.b. BTDF of HOD-500, 2 mm thickness, $\theta_i=30^\circ$, $\theta_s=179^\circ$; $\phi_s=0^\circ$; measured by GSFC and NIST STARR.

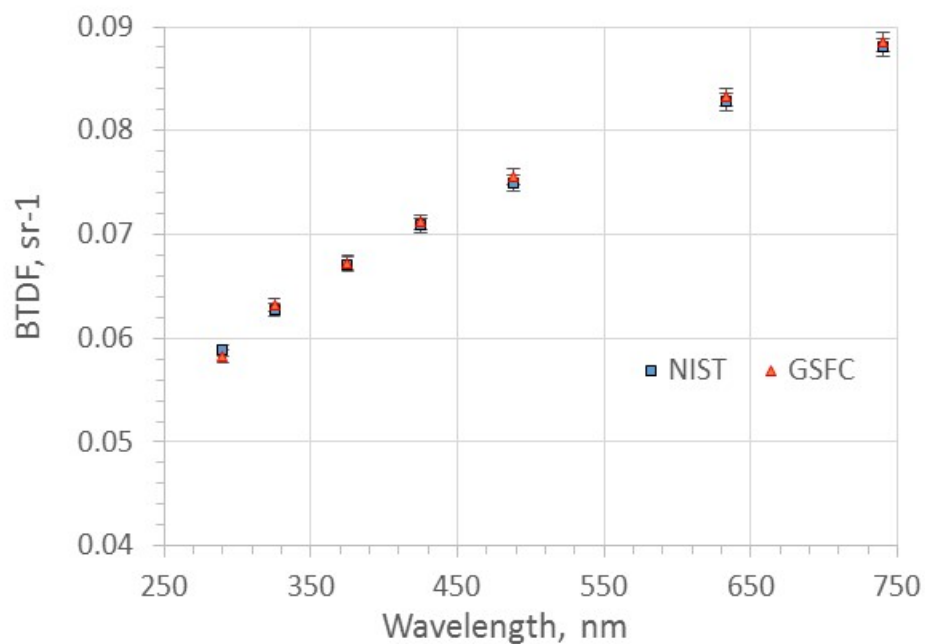


Fig.4.c. BTDF of Spectralon 250 μm thickness, $\theta_i = 0^\circ$, $\theta_s = 179^\circ$; $\phi_s = 0^\circ$; measured by GSFC and NIST STARR.

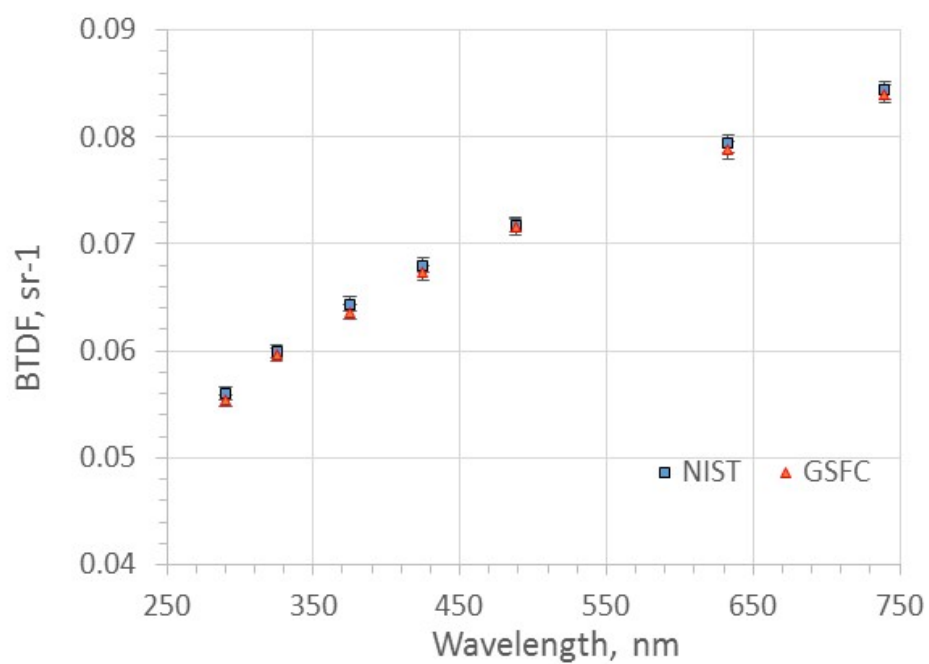


Fig.4.d. BTDF of Spectralon 250 μm thickness, $\theta_i = 30^\circ$, $\theta_s = 179^\circ$; $\phi_s = 0^\circ$; measured by GSFC and NIST STARR

6. UNCERTAINTY

The estimated measurement uncertainty factors for BTDF measurements contribute to a combined measurement uncertainty of less than 1.0% ($k = 1$). The BRDF measurement uncertainty, Δ_{BRDF} , depends on several instrument values⁴ can be evaluated and expressed in accordance with NIST guidelines³ as

$$(\Delta_{BRDF})^2 = 2(\Delta_{NS})^2 + 2(\Delta_{LIN})^2 + (\Delta_{SLD})^2 + (\Delta_{\theta_s} \tan(\theta_s))^2, \quad (5)$$

where Δ_{NS} is the noise to signal ratio, Δ_{LIN} is the non-linearity of the electronics, Δ_{SLD} is the error of the receiver view angle, Δ_{θ_s} is the error of the total scatter angle, and θ_s is the error of the receiver scatter angle. The error of the receiver view angle, Δ_{SLD} , is

$$(\Delta_{SLD})^2 = (2\Delta_{RM})^2 + (2\Delta_{RZ})^2 + (2\Delta_{RA})^2, \quad (6)$$

where Δ_{RM} is the error in the goniometer receiver arm radius, Δ_{RZ} is the error of the receiver arm radius due to sample Z direction misalignment, and Δ_{RA} is the error of the receiver aperture radius. The total scatter angle error, Δ_{θ_s} , is

$$(\Delta_{\theta_s})^2 = (\Delta_{\theta_M})^2 + (\Delta_{\theta_Z})^2 + (\Delta_{\theta_T})^2, \quad (7)$$

where Δ_{θ_M} is the error of the goniometer scatter angle, Δ_{θ_Z} is the error due to sample Z direction misalignment, and Δ_{θ_T} is the sample tilt error.

Uncertainty component	Equation Variable	Uncertainty
1/(Signal to Noise)	Δ_{NS}	0.001
Detector/electronics non-linearity	Δ_{LIN}	0.0035
Receiver solid angle	Δ_{SLD}	0.0032
•Goniometer arm radius	Δ_{RM}	0.0004
•Sample z misalignment	Δ_{RZ}	0.0004
•Detector aperture radius	Δ_{RA}	0.0015
Total scatter angle	Δ_{θ_s}	0.0041
•Goniometer scatter angle	Δ_{θ_M}	0.0023
•Sample z misalignment	Δ_{θ_Z}	0.0005
•Sample tilt error	Δ_{θ_T}	0.0033
NIST lab standard measurement	Δ_{NIST}	0.0056
Total measurement uncertainty ($k=1$)	Δ_{BSDF}	0.0083 or 0.83%

6. CONCLUSIONS

The validation of BTDF calibration capabilities at the Diffuser Calibration Lab of NASA's Goddard Space Flight Center is presented. The Diffuser Calibration Lab participated in BTDF calibration of transmissive diffusers for space applications. The Facility Scatterometer was validated with NIST STARR instrument. The uncertainty budget of 1% was confirmed in the spectral range from 290 nm up to 740 nm. Two laboratory transmissive diffusers were used at this validation, a 2 mm thick Mie quartz diffuser and a 250 μm thick Spectralon diffuser. The validation was performed at incident angles $\theta_i = 0^\circ$ and $\theta_i = 30^\circ$ with $\phi_i = 0^\circ$. The scatter angles were θ_s from 165° to 179° with step of 2° ; ϕ_s was 0° and 180° .

Additional transmissive samples will be measured in the future, keeping in mind the lessons learned during these validation efforts. One lesson learned includes striving to use diffusers in validations with NIST that exhibit BTDFs similar to those used in space or in validation studies. The physical

properties of the diffuser surface has to be very well defined to avoid additional contributions to the overall measurement uncertainty budget.

ACKNOWLEDGEMENTS

The authors gratefully acknowledge the support of Howard Yoon and Thomas Germer of NIST, John Stover of The Scatter Works, Chris Staats of Schmidt Measurement systems , and Gerhard Meister of NASA Goddard Space Flight Center for their encouragement and fruitfully discussions, also John Cooper of Sigma Space Corp. for his consistent laboratory help on measurement setups and discussions.

*Note: Certain commercial equipment, instruments, or materials are identified in this paper in order to specify the experimental procedure adequately. Such identification is not intended to imply recommendation or endorsement by NASA or NIST, nor is it intended to imply that the materials or equipment identified are necessarily the best available for the purpose.

¹ J.J. Butler, B.C. Johnson, R.A. Barnes, "The calibration and characterization of Earth remote sensing and environmental monitoring instruments", in *Optical Radiometry*, Ed. A.C. Parr, R.U. Datla, J.L. Gardner, Academic Press, New York (2005),

² G.T. Georgiev, J.J. Butler, "Laboratory-based Bidirectional reflectance distribution functions of radiometric tarps", *Applied Optics*, **47**, 18, 3313-3323 (2008)

³ Taylor B.N., Kuyatt C. E., "A guidelines for evaluating and expressing the uncertainty of NIST measurement results", NIST Technical Note 1297, U.S. Department of Commerce, National Institute of Standards and Technology, Sep. 1997,

⁴ Schiff T.F., Knighton M.W., Wilson D.J., Cady F.M., Stover J.C., Butler J.J., "A design review of a high accuracy UV to near infrared Scatterometer", *Proc. SPIE*, 1993, **1995**, 121-130,

⁵ Early E.A., Barnes P.Y., Johnson B.C., Butler J.J., Bruegge C.J., Biggar S.F., Spyak P.S., Pavlov M.M., "Bidirectional reflectance round-robin in support of the Earth observing system program", *J. Atmospheric and Oceanic Technology*, 2000, **17**, 1077-1091,

⁶ Georgiev G.T., Butler J.J., "Bidirectional reflectance distribution function and directional-hemispherical reflectance of a Martian regolith simulant", *Optical Engineering*, 2005, **44**, 036202-1-11.

⁷ Nicodemus F.E., Richmond J.C., Hsia J.J., Ginsburg I.W., Limperis T., "Geometrical considerations and nomenclature for reflectance", *National Bureau of Standards, NBS monograph 160*, Oct. 1977,

⁸ Stover J.C., "Optical scattering: measurement and analysis", SPIE Press, Bellingham, Washington, 1995,